New Journal of Physics
The open–access journal for physics

# Turbulent cascades, transfer, and scale interactions in magnetohydrodynamics

**A Alexakis[1,2], P D Mininni[1,3] and A Pouquet[1]**

[1] National Center for Atmospheric Research, P O Box 3000, Boulder, CO 80307, USA
[2] Laboratoire Cassiopée, Observatoire de la Côte d'Azur, BP 4229, Nice Cedex 04, France
E-mail: alexakis@obs-nice.fr, mininni@ucar.edu and pouquet@ucar.edu

*New Journal of Physics* **9** (2007) 298
Received 7 January 2007
Published 31 August 2007
Online at http://www.njp.org/
doi:10.1088/1367-2630/9/8/298

**Abstract.** The nature of the interactions between different scales in magnetohydrodynamic (MHD) turbulence is important for the understanding of the behaviour of magnetized astrophysical, geophysical and industrial flows in a turbulent state. In this paper, we review some recent results in the study of locality of interactions in turbulent flows and we address some of the questions that arise. We examine the cascade of ideal invariants in turbulent MHD flows by examining the transfer functions. We show new results indicating that the nonlocal behaviour of the energy transfer in MHD is the result of a correlation between the velocity and magnetic fields. This nonlocality disappears if we randomize the phases of the two fields keeping the hydrodynamic and magnetic helicities fixed. The cascade of magnetic helicity is also investigated, with special focus on the fate of the small-scale helicity and its coupling with the large-scale flow. These results have implications for dynamo action, in particular for the commonly used distinction between large- and small-scale dynamos. The long-range interactions that exist in MHD flows also raise the question of the existence of universality in MHD, both in the kinematic dynamo regime as well as in the turbulent steady state.

[3] Author to whom any correspondence should be addressed.


PII: S1367-2630(07)41621-4

## Contents



## 1. Introduction

Most of the barionic matter in the universe is in an ionized turbulent state coupled to magnetic fields strong enough to play a dynamical role in the involved processes; e.g. in solar and stellar winds, in accretion disks, and in the interstellar medium. Although in many cases a complete description requires a generalized Ohm's law and the inclusion of kinetic plasma effects [1]–[3], in general the large scales can be properly described by the magnetohydrodynamic (MHD) approximation [4]. Moreover, the Reynolds numbers (the ratio of nonlinear to dissipation terms) in these systems are large and the flows are in a turbulent state. It is essential therefore to understand and quantify the statistical properties of MHD turbulence in order to understand and predict the physical evolution of many astrophysical and geophysical systems.

In the Kolmogorov description of hydrodynamic turbulence, the interactions of similar size eddies play the basic role of cascading the injected energy to smaller scales on a timescale $\tau_l = l/u_l$, where $l$ is the examined length scale and $u_l$ the characteristic velocity at this scale. This procedure persists up to the dissipation length scale where energy is finally dissipated. Imposing a constant energy flux $\epsilon = u_l^2/\tau_l$ at the inertial range leads to the well verified (up to intermittency corrections) scaling $u_l^2 \sim l^{2/3}$, or in spectral space $E(k) \sim k^{-5/3}$. The role of the large-scale flow in this scenario is limited to just advecting the small size eddies without significantly distorting them. One then expects that the resulting structures in scales sufficiently small are independent of the way the system is forced in the large scales and have therefore a universal behaviour.

It has been shown however even for simple hydrodynamic flows in both experiments [5]–[8] and numerical simulations [9, 10] that the large-scale flow still plays an important role in the cascade of energy and the formation of structures in the small scales. In numerical simulations with Reynolds numbers as high as $R_\lambda \sim 800$, it was observed that 20% of the energy flux in the small scales is due to interactions with the large-scale flow. This represents a deviation from self-similarity, and the presence of nonlocal interactions can be associated with clustering of vortex tubes in regions of intense large-scale shear [10], the presence of long-time correlations in the small scales (compared with the eddy turnover time) [8], slower than expected recovery of isotropy [11], and intermittency [12] (which in turn implies corrections to the energy spectrum). Here, $R_\lambda = U\lambda/\nu$ denotes the Reynolds number based on the Taylor lengthscale, defined in the simulations as $\lambda = 2\pi(\int E(k)\mathrm{d}k/\int E(k)k^2\mathrm{d}k)^{1/2}$ ($2\pi$ is the size of the computational domain), $U = \langle u^2\rangle^{1/2}$ is the r.m.s. velocity, and $\nu$ the kinematic viscosity of the fluid.

In MHD flows, the role of the large-scale flow and large-scale magnetic structures is expected to be even more important since the effect of a large-scale magnetic field cannot be 'taken away'

by a Galilean transformation as the velocity in both the hydrodynamic and MHD case. As a result, small scales can interact directly with the large scales and we cannot *a priori* follow the same arguments Kolmogorov used in hydrodynamic turbulence. So assumptions of locality of interactions are in question. Accordingly, some phenomenological models try to take into account the effect of nonlocal interactions assuming a small size eddy interacts strongly with the large-scale magnetic field and the energy cascades on a longer timescale $\tau_l \sim B_0 l/u_l^2$, where $B_0$ is the characteristic amplitude of the magnetic field at the large scales. Assuming a constant flux $\epsilon \sim u_l^2/\tau_l$ leads to the Iroshnikov–Kraichnan scaling $u_l^2 \sim l^{1/2}$ that results in the $k^{-3/2}$ power law for the energy spectrum [13, 14]. Similar phenomenological models that take into account the anisotropy due to the large-scale magnetic field have also been investigated in the literature [15]–[19]. However, although these phenomenological descriptions assume that a large-scale field has the effect of reducing the energy cascade rate, the transfer of energy (and the cascade) still takes place between eddies of similar size, an assumption that needs to be tested.

Before proceeding any further we need to clarify what we mean by local and nonlocal interactions, local and nonlocal transfer, and local and nonlocal cascade of an ideal quadratic invariant. Because of the quadratic form of the nonlinear terms in the incompressible hydrodynamic and MHD equations, three wavenumbers are involved in any basic interaction, with the ideal invariant being transferred between two of the wavenumbers (say $\mathbf{k}$ and $\mathbf{q}$) while the third wavenumber (say $\mathbf{p}$) is responsible for the transfer [20, 21]. Because of the condition $\mathbf{k} + \mathbf{q} + \mathbf{p} = 0$, at least two of the wavenumbers have to be of the same order, while the third can either be of the same order or much smaller than the other two. The interactions for which all three wavenumbers are of the same order are going to be called local, and nonlocal, if otherwise. If the two wavenumbers that exchange energy ($\mathbf{k}$ and $\mathbf{q}$) are of the same order we will talk about local transfer, and nonlocal, if otherwise. Note that locality of interactions implies locality of transfer, but not the other way round. Finally, if in a given flow all interactions are present (both local and nonlocal), we will talk about a local cascade when most of the flux of the invariant is due to local interactions.

'Kolmogorov-like' phenomenological descriptions assume that most of the energy flux is due to local interactions. There are two possible deviations from this local cascade: (i) the transfer of an ideal invariant can be local ($|\mathbf{k}| \sim |q|$) but due to nonlocal interactions ($|\mathbf{p}| \ll |\mathbf{k}| \sim |\mathbf{q}|$), or (ii) the transfer itself can be nonlocal. In the results that we discuss in the following sections both forms of nonlocality are present, but we will focus on the study of the nonlocal transfer. Also, in many of the examined cases both local and nonlocal transfers give contributions to the fluxes. We will refer to both processes as 'cascades' as long as the total flux of the invariant is constant in a range of wavenumbers, to avoid introducing new terminology each time nonlocal transfers appear.

With these definitions in mind we recall some of the recently obtained results in MHD turbulence. Authors [21]–[23] have shown that the locality of energy transfer is in question in MHD flows. In particular, it was demonstrated from simulations that the transfer of energy in MHD has two components: a local one that shares similar properties with hydrodynamic turbulence, and a nonlocal component for which energy from the large scales is injected directly into the small scales without the intervention of the intermediate scales. In dynamo simulations, during the kinematic stage of exponential amplification of magnetic energy (in which the magnetic field is too weak to feedback and modify the flow through the Lorenz force and it is advected and stretched passively) this nonlocal behaviour appears to be even stronger [24, 25].

The nonlocal transfer appears to be even stronger when one investigates the cascade of magnetic helicity. Magnetic helicity is an ideal invariant in MHD that is known to cascade inversely (to the large scales) [26]–[30] in a turbulent flow. The generation of large-scale magnetic fields, for example in galaxies and other astrophysical bodies, is attributed to the inverse cascade of magnetic helicity. Nonlocal transfer of helicity has been observed [30] due to the 'alpha' effect [26, 31, 32], where magnetic energy and helicity are injected in the largest scale of the system directly from the forced scale. Furthermore, nonlocal transfer of helicity has also been observed between the largest scale of the flow and the smallest, even dissipative, scales. This latter process removes magnetic helicity from the large scales, and is attributed to reconnection events that allow the large-scale magnetic field to 'unwind', destroying in that way large-scale magnetic helicity.

Nonlocality appears to be an essential ingredient for a phenomenological understanding and description of MHD turbulence. The following questions then arise: what are the physical processes and structures that result in this nonlocal behaviour? What are the implications on the flow properties and for its modelling? Can we still pursue a unique universal theory that describes MHD turbulence?

In this paper, we review previous results and present a new analysis of the transfer of energy and magnetic helicity in MHD flows. Section 2 introduces the equations and notation, and discusses the transfer of energy in MHD. Evidence of a connection between correlations of the velocity and magnetic fields, and nonlocal transfer of energy is presented. Section 3 considers the transfer of magnetic helicity. The flux of magnetic helicity in Fourier space in mechanically forced simulations is studied in detail, and the coexistence of direct and inverse transfers of helicity in different scales is shown. Section 4 considers the implications of these results for dynamo simulations. In particular, a classification of small- and large-scale dynamos based on the transfer of energy is attempted. Finally, section 5 summarizes the results and discusses the implications for the notion of universality in turbulent MHD flows.

## 2. Energy transfer and structures in MHD turbulence

In the following sections we are going to investigate the incompressible MHD equations with Prandtl number $P_M = 1$ (expressing the ratio of kinematic viscosity $\nu$ to magnetic diffusivity $\eta$). Some cases with $P_M < 1$ will be considered in section 4. The results that are going to be presented are based on direct numerical simulations (DNS) of the MHD equations solved by a dealiased pseudospectral method in triple periodic boxes. No uniform magnetic field is imposed in any of the simulations studied.

The equations that describe the dynamics of an incompressible conducting fluid coupled to a magnetic field in the MHD approximation are given by:

$$\partial_t \mathbf{u} + \mathbf{u} \cdot \nabla \mathbf{u} = -\nabla p + \mathbf{b} \cdot \nabla \mathbf{b} + \nu \nabla^2 \mathbf{u} + \mathbf{f}, \tag{1}$$

$$\partial_t \mathbf{b} + \mathbf{u} \cdot \nabla \mathbf{b} = \mathbf{b} \cdot \nabla \mathbf{u} + \eta \nabla^2 \mathbf{b}, \tag{2}$$

$$\nabla \cdot \mathbf{u} = 0, \quad \nabla \cdot \mathbf{b} = 0, \tag{3}$$

where $\mathbf{u}$ is the velocity field, $\mathbf{b}$ is the magnetic field, and $p$ is the (total) pressure. Here, $\mathbf{f}$ is the external force that drives the turbulence and the dynamo process that sustains magnetic field against Ohmic dissipation.

To investigate the transfer of energy among different scales in a turbulent flow we will introduce the shell filter decomposition of the two fields:

$$\mathbf{u}(\mathbf{x}) = \sum_K \mathbf{u}_K(x), \mathbf{b}(\mathbf{x}) = \sum_K \mathbf{b}_K(x),$$

where

$$\mathbf{u}_K(x) = \sum_{K < |\mathbf{k}| \leqslant K+1} \tilde{\mathbf{u}}(k)\mathrm{e}^{\mathrm{i}\mathbf{k}\mathbf{x}}, \quad \text{and} \quad \mathbf{b}_K(x) = \sum_{K < |\mathbf{k}| \leqslant K+1} \tilde{\mathbf{b}}(k)\mathrm{e}^{\mathrm{i}\mathbf{k}\mathbf{x}},$$

where $\tilde{\mathbf{u}}(k)$ and $\tilde{\mathbf{b}}(k)$ are the Fourier transforms of the two fields with wavenumber $\mathbf{k}$. The fields $\mathbf{u}_K$ and $\mathbf{b}_K$ are therefore defined as the part of the velocity and magnetic field respectively, whose Fourier transform contains only wavenumbers in the shell $(K, K+1]$ (hereafter called the shell $K$). Alternatively, the shells can be defined in a logarithmic binning $(\gamma^n K_0, \gamma^{n+1} K_0]$ for some positive $\gamma > 1$ and integer $n$. However, logarithmic binning cannot distinguish transfer between linearly neighbouring shells ($K$ to $K+1$) from the transfer between logarithmic neighbouring shells ($K$ to $\gamma K$). If in MHD the energy cascade is the result of interactions with the large-scale field (e.g. at the forced scale $k_\mathrm{f}^{-1}$), the energy in a shell $K \gg k_\mathrm{f}$ will be transferred into the shell $K + k_\mathrm{f}$ and logarithmic binning will not be able to distinguish this transfer from the transfer due to local interactions. For this reason, we use linear binning but we note that care needs to be taken when using the word 'scale' that implies in general a logarithmic division of the wavenumbers. The transfer among logarithmic shells can be reconstructed at any time later by summing over the linearly spaced shells.

The evolution of the kinetic energy in a shell $K$, $E_u(K) = \int \mathbf{u}_K^2/2 \, \mathrm{d}x^3$ is given by:

$$\partial_t E_u(K) = \sum_Q [\mathcal{T}_{uu}(Q, K) + \mathcal{T}_{bu}(Q, K)] - \nu \mathcal{D}_u(K) + \mathcal{F}(K), \tag{4}$$

$$\partial_t E_b(K) = \sum_Q [\mathcal{T}_{bb}(Q, K) + \mathcal{T}_{ub}(Q, K)] - \eta \mathcal{D}_b(K). \tag{5}$$

Here we have introduced the functions $\mathcal{F}(K)$, $\mathcal{D}_u(K)$, $\mathcal{D}_b(K)$ that express respectively the energy injection and dissipation in the shell $K$, and the transfer functions $\mathcal{T}_{uu}(Q, K)$, $\mathcal{T}_{ub}(Q, K)$, $\mathcal{T}_{bb}(Q, K)$, and $\mathcal{T}_{bu}(Q, K)$, that express the energy transfer between different fields and shells:

$$\mathcal{T}_{uu}(Q, K) \equiv -\int \mathbf{u_K}(\mathbf{u} \cdot \nabla)\mathbf{u_Q} \, \mathrm{d}\mathbf{x}^3, \quad \mathcal{T}_{bu}(Q, K) \equiv \int \mathbf{u_K}(\mathbf{b} \cdot \nabla)\mathbf{b_Q} \, \mathrm{d}\mathbf{x}^3, \tag{6}$$

$$\mathcal{T}_{bb}(Q, K) \equiv -\int \mathbf{b_K}(\mathbf{u} \cdot \nabla)\mathbf{b_Q} \, \mathrm{d}\mathbf{x}^3, \quad \mathcal{T}_{ub}(Q, K) \equiv \int \mathbf{b_K}(\mathbf{b} \cdot \nabla)\mathbf{u_Q} \, \mathrm{d}\mathbf{x}^3. \tag{7}$$

The function $\mathcal{T}_{uu}(Q, K)$ expresses the transfer rate of kinetic energy lying in the shell $Q$ to kinetic energy lying in the shell $K$, due to the advection term in the momentum equation (1). Similarly, $\mathcal{T}_{bb}(Q, K)$ expresses the rate of energy transfer of magnetic energy lying in the shell $Q$ to magnetic energy lying in the shell $K$ due to the magnetic advection term. The Lorentz force is responsible for the transfer of energy from the magnetic field in shell $Q$ to the velocity

field in the shell $K$, and the resulting transfer function is given by $\mathcal{T}_{bu}(Q, K)$. Finally, the term responsible for the stretching of the magnetic field lines in the induction equation (2) results in the transfer of kinetic energy to magnetic energy, and is expressed by $\mathcal{T}_{ub}(Q, K)$. These transfer functions satisfy

$$\mathcal{T}_{vw}(Q, K) = -\mathcal{T}_{wv}(K, Q). \tag{8}$$

(where $v$, $w$ can be either $u$ and/or $b$). This expression indicates that the rate at which the shell $Q$ gives energy to the shell $K$ is equal to the rate the shell $K$ receives energy from the shell $Q$.

The shell-to-shell energy transfer functions have been studied extensively for a variety of mechanically forced and decaying MHD flows in two and three dimensions, in the saturated turbulent regime and in the kinematic dynamo regime [20]–[22], [25, 33, 34]. Here we present a short summary of the results. In all cases examined in the literature the transfers $\mathcal{T}_{uu}$ and $\mathcal{T}_{bb}$ have a local behaviour: energy is transferred forward between nearby shells, from slightly smaller wavenumbers to slightly larger wavenumbers. This is similar to what is measured in hydrodynamic turbulence [9, 10], [35]–[38]. On the other hand, the transfers $\mathcal{T}_{bu}$ and $\mathcal{T}_{ub}$, that express the energy exchange between the two different fields, have a rather different behaviour. The magnetic field in a shell $K$ receives energy at the same rate from all wavenumbers smaller than $K$, and gives energy to shells with slightly larger wavenumbers. In addition, when the system is mechanically forced there is a strong input of magnetic energy directly from the forced scale to all shells [21, 23, 34]. This kind of transfer is absent in free decaying runs [22]. We note that in mechanically forced runs, the velocity field has to supply energy to the magnetic field all the time in order to sustain the magnetic field against Ohmic dissipation. This is not necessarily true for freely decaying runs where both fields are dissipated in time. As a result, some differences can be expected in the transfer function of mechanically forced dynamos, free decaying runs, and electrically forced flows (not examined here).

A natural question to ask is: why the transfer between two different fields (expressed by the functions $\mathcal{T}_{bu}$ and $\mathcal{T}_{ub}$) is so different than the transfers among the same field ($\mathcal{T}_{uu}$ and $\mathcal{T}_{bb}$)? The answer we will support in the present paper is that correlations between the velocity field and magnetic field make shells of widely separated wavenumbers efficient for the transfer of energy. To support this claim we compare the energy transfer of two different sets of velocity and magnetic fields ($\mathbf{u}$, $\mathbf{b}$). The first set ($\mathbf{u_1}$, $\mathbf{b_1}$) comes from a (numerical) solution of the MHD equations: a turbulent MHD flow resulting from a saturated dynamo simulation with ABC (helical) forcing acting at the wavenumber $k_f \approx 3$. The Reynolds numbers of the flow are $R_e = R_m \approx 820$ with $R_e = UL/\nu$ and $R_m = UL/\eta$ the mechanical and magnetic Reynolds numbers respectively, based on the integral scale of the flow $L = 2\pi(\int E(k)k^{-1}\mathrm{d}k/\int E(k)\mathrm{d}k)$. The simulation was done on a $256^3$ grid. The second set of fields ($\mathbf{u_2}$, $\mathbf{b_2}$) was created by taking the first set and randomizing the phases of each Fourier coefficient under the procedure $\tilde{\mathbf{u}}_2(\mathbf{k}) = \mathrm{e}^{\mathrm{i}\phi_\mathbf{k}}\tilde{\mathbf{u}}_1(\mathbf{k})$ and $\tilde{\mathbf{b}}_2(\mathbf{k}) = \mathrm{e}^{\mathrm{i}\psi_\mathbf{k}}\tilde{\mathbf{b}}_1(\mathbf{k})$, where $\phi_\mathbf{k}$ and $\psi_\mathbf{k}$ are random numbers that depend only on the wavenumber $\mathbf{k}$. In this way, incompressibility of each field, the kinetic and magnetic energy spectra, and the kinetic and magnetic helicities remain unchanged. However, the cross helicity of the two fields can change, which is a desired effect since we want to destroy correlations between the fields and their modes. In practice, five different realizations were used for the fields ($\mathbf{u_2}$, $\mathbf{b_2}$). Each realization was obtained by applying a different sequence of random phases to the fields ($\mathbf{u_1}$, $\mathbf{b_1}$). The transfers resulting from each realization were averaged at the end.

A cross-section of the $z$-component of the current density ($j_z$, with $\mathbf{j} = \nabla \times \mathbf{b}$) for the two sets is shown in figure 1. The thin filaments with strong current that appear in the right panel

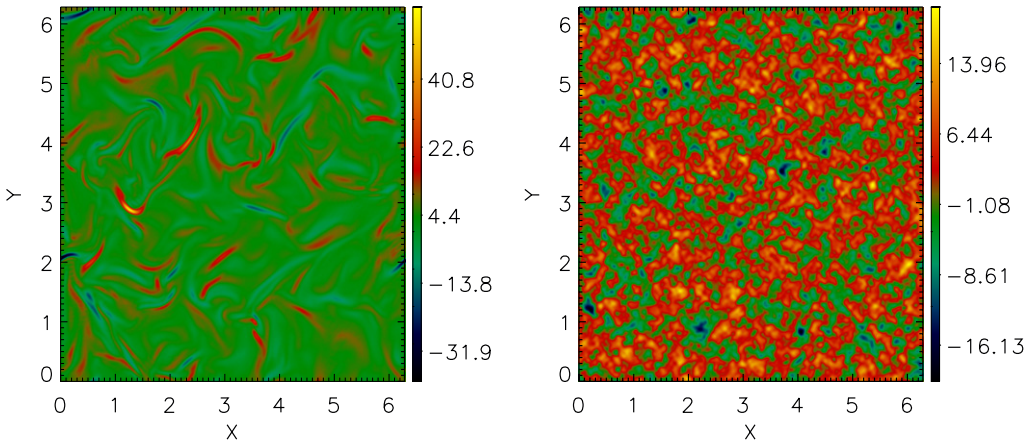


**Figure 1.** Cross-section showing the $z$-component of the current density on the $x$–$y$ plane in the MHD simulation (left) and in the set after randomizing phases in Fourier space (right). Note that thin filaments in the cross-section, associated with current sheets in the 3D flow, have disappeared in the right panel.

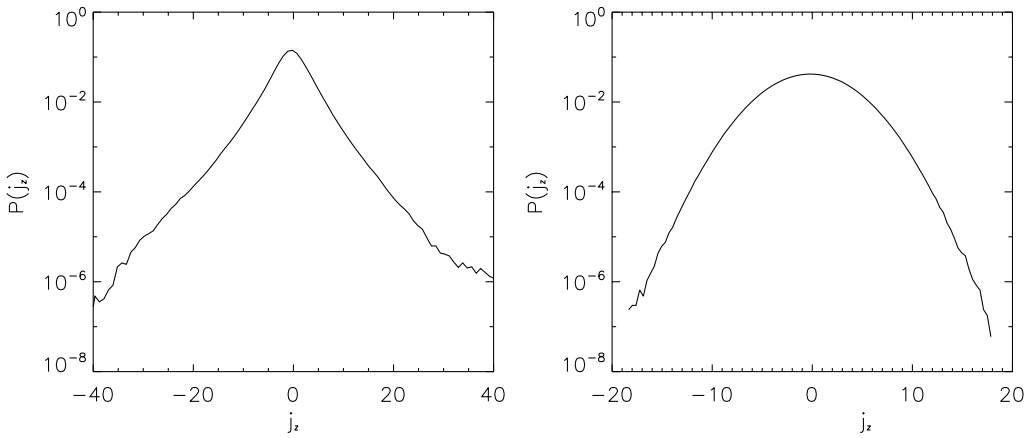


**Figure 2.** Probability density function of the $z$-component of the current density for the magnetic field $\mathbf{b_1}$ from the numerical simulation (left panel), and for the magnetic field $\mathbf{b_2}$ after randomizing phases (right panel).

(resulting from the numerical solution of the MHD equations) are associated with cross-sections of current sheets in the three-dimensional (3D) box. The right panel shows the same cross-section for the randomized magnetic field. In this case the thin filaments have disappeared. Figure 2 shows the probability density function of $j_z$ for the two sets. The stretched exponential distribution with strong tails denoting intermittency that results from the magnetic field $\mathbf{b_1}$ stemming from the numerical simulation (left panel), transforms into a Gaussian distribution for the randomized field $\mathbf{b_2}$ (right panel).

Using these two sets the transfer functions were calculated. Figure 3 shows $\mathcal{T}_{uu}(Q, K)$ and $\mathcal{T}_{ub}(Q, K)$ for a fixed value of $K = 25$. The solid line shows the transfer functions for the solution of the MHD equations $(\mathbf{u_1}, \mathbf{b_1})$, and the dashed line shows the same transfers for the random phased fields $(\mathbf{u_2}, \mathbf{b_2})$. Although the transfers for the random phased fields are noisier, the shape

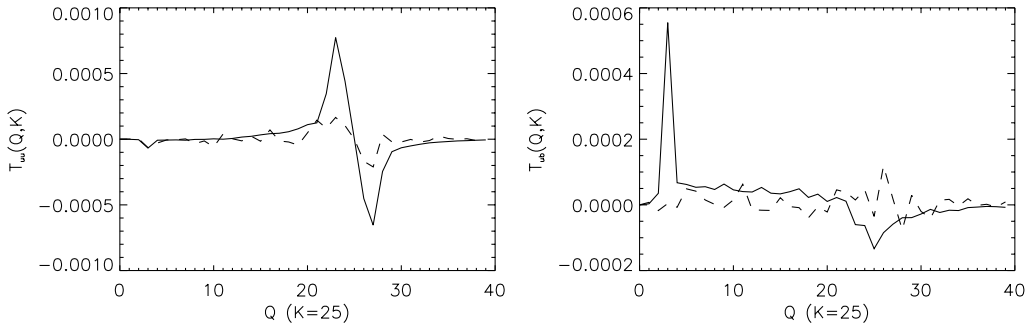


**Figure 3.** Transfer functions $\mathcal{T}_{uu}$ (left panel) and $\mathcal{T}_{ub}$ (right panel) at a fixed value of $K = 25$ for the velocity and magnetic field stemming from a numerical simulation $(\mathbf{u_1}, \mathbf{b_1})$ (solid lines) and for the set with randomized phases $(\mathbf{u_2}, \mathbf{b_2})$ (dashed lines).

of the $\mathcal{T}_{uu}$ transfer is similar to the $(\mathbf{u_1}, \mathbf{b_1})$ set: most of the transfer results from nearby shells. This is expressed in the solid and dashed lines in the left panel of figure 3 by the positive peak to the left of $Q = K = 25$, and by the negative peak to the right of $Q = K = 25$ in $\mathcal{T}_{uu}(Q, K)$. The negative peak in $\mathcal{T}_{uu}$ expresses kinetic energy is taken from wavenumbers $Q$ slightly smaller than $K = 25$, while the positive peak denotes kinetic energy is given to wavenumbers $Q$ slightly larger than $K = 25$. The transfer of kinetic energy due to the advection term in the momentum equation (1) is as a result local and direct, for both sets $(\mathbf{u_1}, \mathbf{b_1})$ and $(\mathbf{u_2}, \mathbf{b_2})$. The fact that the amplitude of the transfer functions is smaller for $(\mathbf{u_2}, \mathbf{b_2})$ probably reflects that the fields with randomized phases being less intermittent, third order quantities in the fields (as the energy flux and transfers) are smaller.

The transfer $\mathcal{T}_{ub}$ behaves differently. For $(\mathbf{u_1}, \mathbf{b_1})$, $\mathcal{T}_{ub}$ peaks at $Q \approx 3$, where mechanical energy is injected by the external forcing, and it is positive for all wavenumbers $0 < Q < K = 25$ (the 'plateau'). This expresses the result previously discussed. In mechanically forced MHD flows, kinetic energy is transferred directly from the forced scale and all shells with wavenumbers $Q < K$ to magnetic energy at each shell $K$. The negative peak in $\mathcal{T}_{ub}$ for $Q > K = 25$ indicates magnetic energy is transferred to kinetic energy at slightly larger wavenumbers. The function $\mathcal{T}_{ub}(Q, K)$ is highly nonlocal for the set $(\mathbf{u_1}, \mathbf{b_1})$. However, for the set $(\mathbf{u_2}, \mathbf{b_2})$ the transfer of energy from the forced wavenumber $Q \approx 3$ to the examined shell $K = 25$ disappears, as well as the plateau. Most of the transfer is local but not clearly forward.

The difference in the transfer of the two fields can also be seen in figure 4 where a shadowgraph plot of $\mathcal{T}_{ub}$ is shown. The nonlocal input of energy from the forced large-scale to the magnetic field at all scales, indicated by the horizontal red-green line (left panel) is absent in the case with randomized phases (right panel). Off-diagonal transfers also disappear in the $(\mathbf{u_2}, \mathbf{b_2})$ set, and for this set most of the $\mathcal{T}_{bu}$ transfer is concentrated close to the diagonal in the $(Q, K)$ plane. Note this transfer function does not have to be antisymmetric with respect to $K$ and $Q$ (see equation (8)).

We conclude that phase correlations for each field as well as correlations between the two fields (velocity and magnetic fields) are important for the transfer, and a simple estimate of the amplitude of the velocity and magnetic field at different scales (i.e. as used in Kolmogorov phenomenology) is not sufficient to estimate the magnitude of the nonlinear terms. We note that

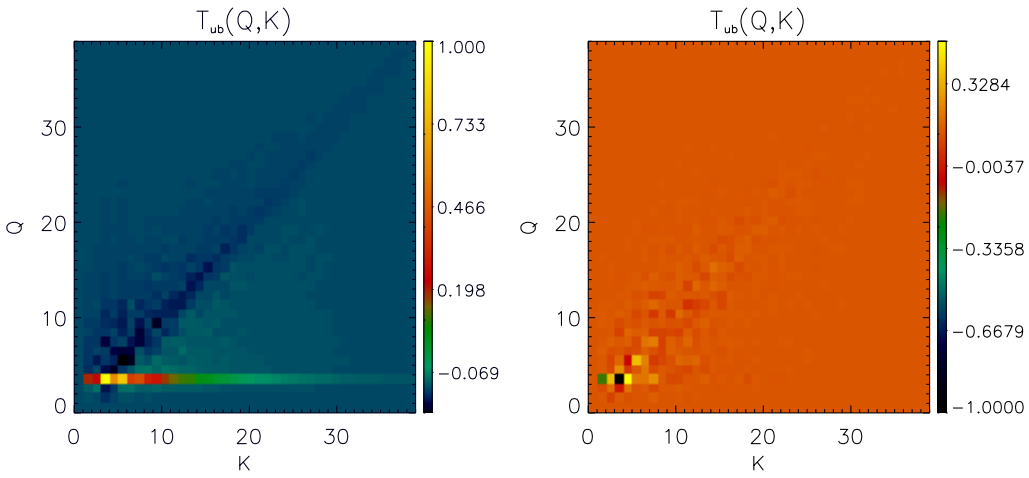


**Figure 4.** Transfer function $\mathcal{T}_{ub}(Q, K)$ (from kinetic energy in the shell $Q$ to magnetic energy in the shell $K$) for the velocity and magnetic field stemming from a DNS ($\mathbf{u_1}$, $\mathbf{b_1}$) (left panel) and for the set with randomized phases ($\mathbf{u_2}$, $\mathbf{b_2}$) (right panel). The amplitude of both transfers was normalized to the maximum of $|\mathcal{T}_{ub}(Q, K)|$.

the correlation between velocity and magnetic fields is also known to be of importance for the energy cascade when a strong guiding field is present [39].

## 3. Magnetic helicity cascade

Besides the evolution of the energy, the evolution of magnetic helicity can also play an important role in the dynamics of an MHD system. Early studies using mean-field theory [31, 32], discrete scale models [40, 41], and turbulent closure models [26, 42] have shown within the framework of the approximations made that magnetic helicity cascades inversely from small scales to large scales. DNS [27]–[29], [43, 44] have verified the inverse transfer and/or cascade of magnetic helicity, as well as the generation of large-scale magnetic fields from small-scale helical forcing. To this inverse cascade of helicity are attributed the large-scale magnetic fields observed in many astrophysical objects. Magnetic helicity is also observed in the solar photosphere in association with coronal mass ejections (CMEs) and sigmoids [45]–[49].

Typically, in numerical investigations of the inverse cascade of magnetic helicity, the flow is forced with a mechanical helical forcing at some intermediate scale, and after the system has reached a hydrodynamic turbulent steady state a small seed magnetic field is introduced (a 'dynamo simulation', as discussed in more detail in the next section). The stretching of the magnetic field lines by the helical flow amplifies the magnetic energy. The process also creates magnetic helicity of the same sign than the kinetic helicity in scales smaller than the forced scales, and magnetic helicity of the opposite sign in the larger scales. As the magnetic field grows stronger and the Lorentz force feeds back on to the flow, the magnetic helicity at the large scales cascades inversely to even larger scales until the largest scale of the system is reached. After this point the magnetic helicity and energy in the largest scale keeps growing possibly until magnetic diffusivity becomes important and saturates the growth [28].

The fate of the small-scale helicity has not been investigated as much. However, in large Reynolds number flows it is important to know if the small-scale magnetic helicity cascades also to larger scales (in which case it will pile up close to the forced scale or cancel some of the magnetic helicity of opposite sign in the large scales), or if it is transferred to smaller scales where it can be destroyed by the magnetic diffusivity. In the former case, no net generation of magnetic helicity exists in the limit of infinite magnetic Reynolds number since both signs of helicity cancel. In the latter case, the small-scale helicity is dissipated even in the limit of infinite magnetic Reynolds number, and the sign of the magnetic helicity in the large-scale prevails. To find the direction of the cascade of helicity one has to determine the sign of the helicity flux

$$\Pi_{\mathrm{H}}(K) = \int \mathbf{b}_K^{<} \cdot (\mathbf{u} \times \mathbf{b})\, \mathrm{d}x^3, \tag{9}$$

where $\mathbf{b}_K^{<}$ is the magnetic field filtered so that only the wavenumbers in the range $0 < |\mathbf{k}| < K$ are kept (not to be confused with the band-pass filtered $\mathbf{b}$ field $\mathbf{b}_K$ defined in the previous section). If the flux of helicity remains of the same sign for all wavenumbers the two signs of helicity cascade in opposite directions. If however both the small-scale positive helicity and the large-scale negative helicity cascade to large scales the flux of helicity will change sign close to the forcing scale.

A detailed examination of the cascading process of magnetic helicity in mechanically and electrically forced flows was investigated in [30], where its transfer rate among different scales was measured from DNS. In the examined runs with mechanical forcing, a positive helical forcing was applied at intermediate scales so that enough large scales were available for an inverse cascade of magnetic helicity to develop. This election naturally limits the Reynolds numbers that can be resolved, and as a result only moderate Reynolds numbers were considered and scales smaller than the forcing scale could not be considered as inertial range scales. In this work we re-examine the same run (with forcing at $k_{\mathrm{f}} \approx 10$ and a spatial resolution of $256^3$ grid points) along with a run forced with the same (positive) sign of kinetic helicity but at larger scales ($k_{\mathrm{f}} \approx 3$ and the same spatial resolution) to investigate the evolution of the magnetic helicity in the small scales with better scale separation. The corresponding Reynolds numbers are $R_e = R_m \approx 240$ in the run forced at $k_{\mathrm{f}} \approx 10$, and $R_e = R_m \approx 820$ in the run forced at $k_{\mathrm{f}} \approx 3$.

The magnetic helicity spectrum for the run forced at $k_{\mathrm{f}} \approx 3$ is shown in figure 5 (left panel) along with the magnetic helicity flux (right panel) for several different times (the first time is before the magnetic helicity spectrum peaks at the largest scale, and the latter is after the spectrum peaks at the largest scale). For comparison we also show the magnetic helicity spectrum and flux for the run forced at $k_{\mathrm{f}} \approx 10$ in figure 6. Clearly the flux remains of the same sign for all scales in both cases, even though the magnetic helicity changes sign at $k \sim k_{\mathrm{f}}$. This implies a different cascade direction for the two signs of magnetic helicity, i.e. that negative helicity (mostly concentrated at the large scales) cascades to larger scales, or equivalently that positive helicity (mostly concentrated at scales smaller then the forcing scale) cascades to smaller scales. As a result, positive helicity cascading forward in scales smaller than the forcing scale, will dissipate when the dissipative scales are reached. At late times the negative magnetic helicity in the large scales will dominate.

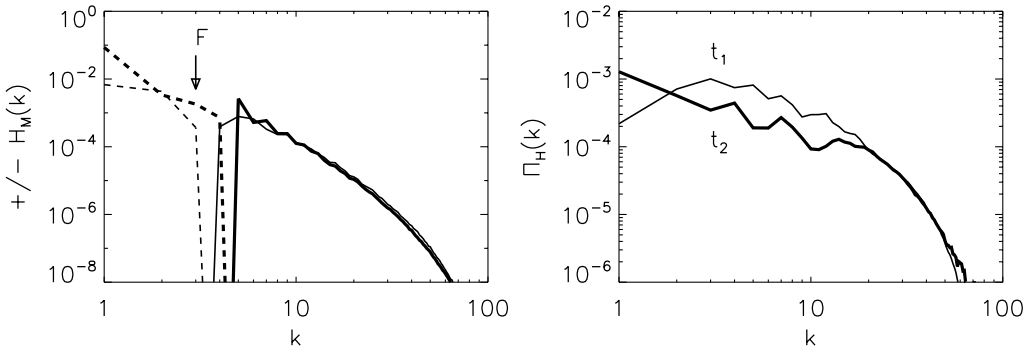


**Figure 5.** Magnetic helicity spectrum (left panel) and flux (right panel) for the run forced at $k_f \approx 3$. Solid lines correspond to positive sign of helicity and flux, while dashed lines correspond to negative sign. The forcing wavenumber is indicated on the left by the arrow. Two different times are shown, before magnetic helicity peaks at $k = 1$ and after the helicity peaks at the largest available scale.

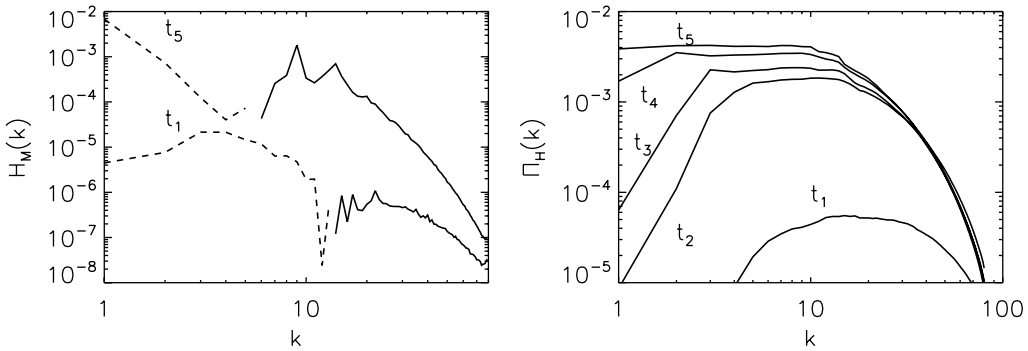


**Figure 6.** Magnetic helicity spectrum (left panel) and flux (right panel) for the run forced at $k_f \approx 10$. Same labels as in figure 5. On the left panel, two different times are shown, before magnetic helicity peaks at $k = 1$ and after the helicity peaks at the largest available scale. On the right panel, five curves indicating the evolution of the flux are shown, including at intermediate times.

The transfer rate of magnetic helicity at shell $Q$ into magnetic helicity at shell $K$ is defined as:

$$\mathcal{T}_h(Q, K) = \int \mathbf{b}_K \cdot (\mathbf{u} \times \mathbf{b}_Q) \mathrm{d}\mathbf{x}^3. \tag{10}$$

The function $\mathcal{T}_h(Q, K)$ expresses the transfer rate of positive helicity from the shell $Q$ to the shell $K$, or equivalently the transfer rate of negative helicity from the shell $K$ into the shell $Q$. Positive values of $\mathcal{T}_h(Q, K)$ imply that positive magnetic helicity is transferred from the shell $Q$ to the shell $K$, while negative values imply the reverse transfer. The terms responsible for this transfer are conservative and do not generate or destroy total magnetic helicity. These terms are responsible only for the redistribution of magnetic helicity among different scales. This fact is expressed by the antisymmetric property of $\mathcal{T}_h(Q, K)$:

$$\mathcal{T}_h(K, Q) = -\mathcal{T}_h(Q, K). \tag{11}$$

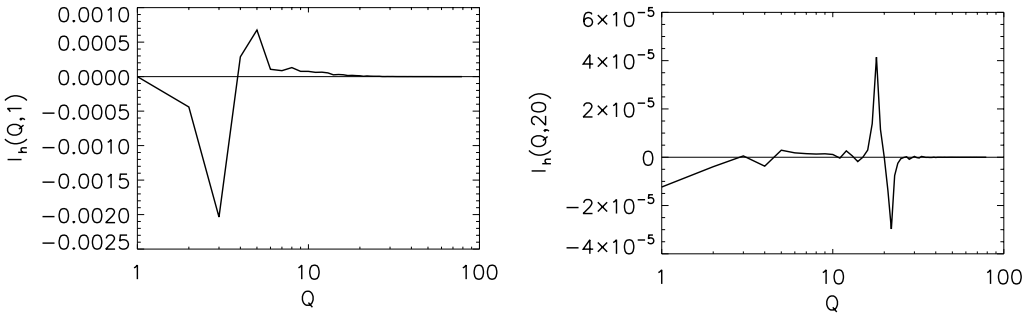


**Figure 7.** Magnetic helicity transfer function $\mathcal{T}_h(Q, K)$ for $K = 1$ (left panel) and $K = 20$ (right panel) in a simulation with helical mechanical forcing acting at $k_f \approx 3$.

We stress that magnetic helicity (unlike energy) is not a positive definite quantity and care needs to be taken when results are interpreted. The analysis of the run forced at smaller scales ($k_f \approx 10$) showed that the magnetic helicity cascade has (superposed to a local inverse transfer) a strongly nonlocal behaviour in two different ways. Firstly, there is a direct input of magnetic helicity from the forced scale directly into the largest scale of the system, that increases as a result of the absolute value of the magnetic helicity at the largest scales. Secondly, there is transfer of helicity from the large (negative) helical scales to the small 'dissipative' (positive) helical scales, destroying as a result both the large-scale positive helicity and the small-scale negative helicity. We note however that for this run the Reynolds number was small and the scales smaller than that of forcing were close to the viscous cut off.

For this reason, we examine here the run forced at larger scales ($k_f \approx 3$). This run has only a few wavenumbers for the inverse cascade of magnetic helicity to develop, but allows us to examine in more detail the dynamics of the magnetic helicity in the small scales. In figure 7 the transfer function $\mathcal{T}_h(Q, K)$ is shown for two different values of $K$. The left panel shows transfer for $K = 1$ (this shell is dominated by negative magnetic helicity, see the spectrum in figure 5). The figure demonstrates that the largest scale of the system receives negative helicity from the forced scale $k_f \sim 3$ (note the negative peak of $\mathcal{T}_h$ for $Q \approx 3$) while at the same time it is 'losing' negative magnetic helicity to the small scales (indicated by the positive values of $\mathcal{T}_h$ for $Q > 3$). In the right panel we show the transfer of helicity for the shell $K = 20$ (a shell with positive magnetic helicity). As it can be seen, there are two components in the transfer. Firstly, there is a local direct transfer of the positive magnetic helicity, i.e. the shell $K = 20$ receives magnetic helicity from slightly smaller wavenumbers and gives magnetic helicity to slightly larger wavenumbers (note the two peaks close to $Q \approx K = 20$). Secondly, there is a negative transfer of magnetic helicity from the shell $K = 20$ to the $Q = 1$ shell. This transfer is highly nonlocal and it is of the same order of magnitude than the local component of the transfer. This nonlocal contribution is probably related to reconnection events that allow the large- and small-scale magnetic fields to unwind by a change of topology in the magnetic field lines.

What determines the saturation amplitude of the large-scale magnetic helicity? If the saturated large-scale field is the result of a balance between the magnetic diffusivity at the large scales $L$ and the forcing $F$ that injects helicity and energy at intermediate scales, the

amplitude of the magnetic field at large-scale $B_0$ should scale like $B_0 \sim FL^2/\eta$ which is very large. If however the non-local transfer of magnetic helicity is efficient enough to destroy large-scale helicity, saturation can be reached for smaller amplitudes of $B_0$ (we note that in physical systems there is also expulsion of magnetic helicity from outflows that helps saturation of the large-scale magnetic field at smaller values). Of course an investigation of the saturation value of the magnetic field in helical flows and its scaling with the magnetic Reynolds and magnetic Prandtl numbers requires long (on the order of diffusive timescales) and high resolution runs, that are numerically too expensive to be investigated yet. It is likely however that the saturation amplitude of the large-scale magnetic field will depend on the way magnetic field lines reconnect in the small scales. It has been shown for example in [2] that the inclusion of the Hall effect (a term that acts on small scales) can increase substantially the saturation amplitude of the magnetic field in the large scales.

The observed direct transfer of magnetic helicity in scales smaller than the forcing scale has also implications for estimations of the diffusion time of the small-scale magnetic helicity [50], and numerical and theoretical studies of the saturation of the $\alpha$-effect in helical dynamos [28, 40, 41, 51]. Many models assume there is an inverse cascade of magnetic helicity at all scales, and as a result the small-scale magnetic helicity for very large magnetic Reynolds numbers should cancel part of the large-scale magnetic helicity. However when the small-scale magnetic helicity is transferred forward to small scales, it can be dissipated very fast (compared with the large-scale magnetic helicity). As a result, estimations of helicity production rates based on an inverse transfer at all scales should be revisited (see [30] for more details).

## 4. Large- and small-scale dynamos

The machinery to quantify transfer of ideal invariants between shells discussed in the previous sections can also be useful to determine what scales are involved in the amplification of the magnetic field during the kinematic stage of dynamos. Dynamos are often classified according to the scales in which magnetic energy is amplified: large- and small-scale dynamos, where large and small is often defined relative to the energy containing scale of the turbulent hydrodynamic flow [51, 52]. Large-scale dynamos are often associated to helical flows, or to anisotropic and inhomogeneous flows (e.g. with a large-scale shear) [26]–[29], [44]. In large-scale dynamos (e.g. in mean field dynamos [31, 32]) the growth rate of the magnetic energy is in general a function of the wavenumber. In the mean field dynamo description the generation of large-scale magnetic fields (see e.g. [52]) in a turbulent flow requires the existence of small-scale fields, since the sources of magnetic energy in the large scales depend on the properties of the small-scale fields if the transfer of $H_M$ is nonlocal.

Small-scale dynamos, in which magnetic fields are correlated at scales smaller than the integral scale of the flow, are often studied for magnetic Prandtl numbers $P_M > 1$ as found in the interstellar medium; nonhelical flows, and delta-correlated in time mechanical forcing are generally assumed [21, 53, 54]. Since when $\nu > \eta$ velocity fluctuations are damped fast in the subviscous scales and the magnetic energy can grow during the kinematic dynamo regime in scales were velocity fluctuations are negligible, it is clear in this case that dynamo action in the subviscous scales takes place through a nonlocal process [24, 55, 56]. In the small mechanical Reynolds number case the velocity field in the large-scales amplifies directly the magnetic energy in all scales, and the magnetic fields at all wavenumbers grow with the same growth rate. The

magnetic energy spectrum at early times has a positive slope $\sim k^{3/2}$ [57] which precludes just a direct local transfer of magnetic energy to the small scales.

The classification of large- and small-scale dynamos is however not so straightforward for the $P_M \leqslant 1$ case, typical of liquid metals in the laboratory, in the Earth's core, or in the solar convection zone. In that case, magnetic energy grows in scales that are larger than the energy containing scale (the large-scale dynamo) and/or scales closer to the resistive scale (the small-scale dynamo). For $R_M$ large enough, the resistive scale can be expected to be in the velocity field inertial range. In this case, 'small scales' for the magnetic fluctuations should be understood as scales smaller than the energy containing scale down to the magnetic diffusion scale. Since $P_M \leqslant 1$, velocity fluctuations can exist at scales much smaller than these scales.

Simulations with helical or nonhelical coherent forcing obtained dynamos [58]–[60] for small magnetic Prandtl numbers down to $P_M \approx 5 \times 10^{-3}$, using a combination of DNS and subgrid-scale modelling. For $P_M \leqslant 1$, the asymptotic value of the critical magnetic Reynolds number for the dynamo instability for nonhelical coherent forcing was found to be more than ten times larger than for helical large-scale dynamos [60], in agreement with theoretical arguments and mean-field models [61]. In all these simulations and for magnetic Reynolds numbers large enough ($R_m \approx 300$), a spectrum $\sim k^{3/2}$ for the magnetic energy at early times was observed, but at late times (i.e. after the nonlinear saturation of the small magnetic scales [62]) the magnetic energy grows at scales larger than the energy containing scale of the flow. However, for helical forcing and small magnetic Reynolds ($R_m \approx 40$) the magnetic energy spectrum peaks at the largest scale at all times. Simulations using delta-correlated in time mechanical forcing obtained a dynamo in the same limit very recently using hyper-viscosity [63, 64], and critical magnetic Reynolds numbers for this forcing were found to be even larger than for nonhelical coherent forcing (see [65, 66] for theoretical studies of the critical magnetic Reynolds number for delta-correlated in time velocity fields when $P_M < 1$).

The different behaviours reported for different forcing functions, and the different properties of the magnetic energy spectrum raise several questions. When is dynamo action in the $P_M < 1$ case of the large- or small-scale type? If both dynamos coexist, can they be distinguished? Or are the two intrinsically linked? What are the sources of the magnetic field: the velocity field in the large scales, the velocity fluctuations, or both? For $P_M \leqslant 1$, are magnetic fluctuations in the small scales sustained by dynamo action, by stretching of the large-scale magnetic field, or by the direct cascade of magnetic energy at the large scales?

The examination of the transfers functions $\mathcal{T}_{ub}(Q, K)$ and $\mathcal{T}_{bu}(Q, K)$ can be used to answer some of these questions. Indeed, these functions measure the amount of work the velocity field in shell $Q$ does to the magnetic field in shell $K$ and vice versa. $Q$-shells with positive $\mathcal{T}_{ub}(Q, K)$ stretch and amplify magnetic energy in shell $K$. On the other hand, the amount of magnetic energy in shell $K$ received from other shells $Q$ due to the direct cascade of energy is measured by the transfer $\mathcal{T}_{bb}(Q, K)$. These transfer functions plus the magnetic dissipation function $\mathcal{D}_b(K)$ (see equation (5)) can be used to define and compute the growth rate of each individual shell in dynamo simulations, as was done for helical and nonhelical forcings in [25] (see also [67]).

In this section we compare the transfers $\mathcal{T}_{ub}$ and $\mathcal{T}_{bb}$ for two $256^3$ dynamo simulations with ABC forcing acting at $k_f \approx 3$, and with $R_m \approx 40$ and $R_m \approx 400$ respectively; $R_e \approx 820$ in both runs which therefore differ in their magnetic Prandtl number by a factor 10. Figure 8 (left panel) shows the transfer $\mathcal{T}_{ub}$ for $K = 20$ for both runs. As previously noted, this function expresses the amount of work the velocity field in shells $Q$ does to the magnetic field in the shell $K$, and

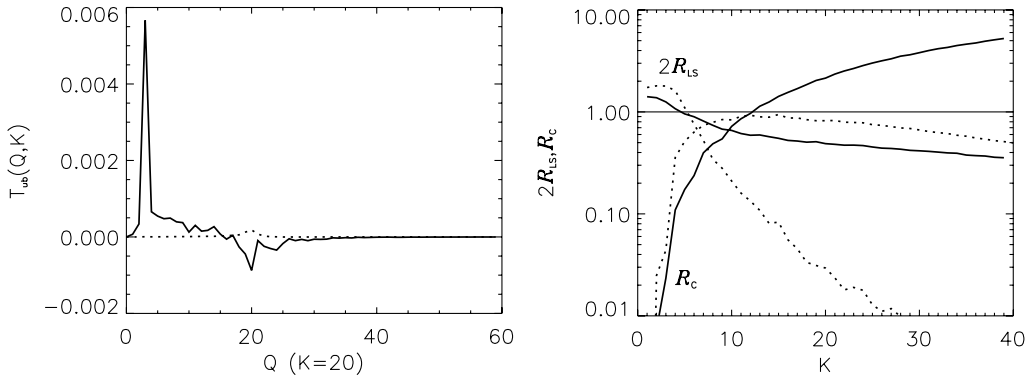


**Figure 8.** Left panel: transfer function $\mathcal{T}_{ub}(Q, K)$ for $K = 20$ in the dynamo simulations with $R_m \approx 400$ (solid) and $R_m \approx 40$ (dashed). The transfer function for this run is small and has been multiplied by a factor of 100 for visualization purposes. Right panel: ratios $\mathcal{R}_{\rm LS}(K)$ and $\mathcal{R}_{\rm C}(K)$ (see text) for the same runs, labels are as in the left panel.

is associated with the term in the induction equation responsible for the stretching of magnetic field lines. In the run with $R_m \approx 40$ there is no nonlocal transfer of kinetic to magnetic energy: the function $\mathcal{T}_{ub}$ for large $K$ only shows a small local transfer between shells $Q \approx K$. Since $R_e \gg R_m \approx 40$ and $Q \approx K$, this can be understood as tangling of the large-scale magnetic field (in shells $P \ll Q \approx K$) by turbulent fluctuations in the shell $Q \approx K$ (see e.g. [68]). The magnetic energy injected into these sub-resistive scales is then rapidly dissipated. At small wavenumbers $Q < 5$, the magnetic field is mostly fed by the large-scale flow at $k_{\rm f}$ (not shown). On the other hand, the run with $R_m \approx 400$ shows nonlocal transfer of kinetic energy from the forced scale to all magnetic scales (see the positive peak at $Q \approx k_{\rm f}$) and the transfer from velocity fluctuations at all scales (the positive plateau) is also present. Both the peak at $Q \approx k_{\rm f}$ and the portion of the plateau with $Q < K$ describe stretching of small-scale magnetic fields in shells $P \approx Q$, since the relation $\mathbf{k} + \mathbf{p} + \mathbf{q} = 0$ indicates that only the velocity in the shell $Q \approx K$ can stretch large-scale magnetic field ($P \approx 1$) and transfer that energy to the magnetic shell $K$.

The relative importance of each transfer is further illustrated by the right panel in figure 8, which shows the ratios

$$\mathcal{R}_{\rm LS}(K) = \sum_{Q=2,3,4} \mathcal{T}_{ub}(Q, K) \Big/ \sum_{Q} \mathcal{T}_{ub}(Q, K), \tag{12}$$

and

$$\mathcal{R}_{\rm C}(K) = \sum_{Q=0}^{K} \mathcal{T}_{bb}(Q, K) \Big/ \sum_{Q} \mathcal{T}_{ub}(Q, K). \tag{13}$$

Equation (12) is the ratio of energy a magnetic shell $K$ receives only from the large-scale flow (the peak at $Q \approx 3$ in the left panel of figure 8) to the total energy received by the shell $K$ from the velocity field at all shells. Equation (13) is the ratio of energy a magnetic shell $K$ receives

from the direct transfer of magnetic energy from larger scales to the total energy received in the same shell from the velocity field by stretching of field lines.

In the run with $R_m \approx 40$, the large-scale velocity field is the dominant source of magnetic energy for shells up to $K \approx 5$. For $K \leqslant 5$ the ratio $\mathcal{R}_C(K)$ turns rapidly of order one and stays there for all magnetically excited scales. As a result, the small-scale magnetic fluctuations in scales smaller than the energy containing scale of the flow are mostly due to the direct transfer of magnetic energy. As the magnetic Reynolds number is increased, these results change. In the run with $R_m \approx 400$, the large-scale magnetic field is still sustained by the large-scale flow. But for $K \leqslant 5$ the ratio $\mathcal{R}_C(K)$ grows more slowly than in the $R_m \approx 40$ run, and is smaller than one up to $K \approx 10$. In these intermediate scales, stretching of magnetic field lines by the large-scale flow and by the turbulent fluctuations is dominant over the direct transfer of magnetic energy.

While both runs sustain dynamo action, in the run with $R_M \approx 40$ only the large-scale magnetic field grows due to dynamo action. In the small-scales, magnetic energy is small and mostly fed by the direct cascade of energy. As the magnetic Reynolds number is increased, stretching of field lines in scales smaller than the energy containing scale turns to be dominant over the direct transfer of magnetic energy, and an intermediate range of scales appears where scales are excited by small-scale dynamo action. This effect is accompanied by the development of the magnetic energy spectrum $\sim k^{3/2}$ at early times. It is worth noticing that in these simulations, the small-scale dynamo can be fed by two sources: the large-scale flow (which is unsteady, since fluctuations in a turbulent flow are present at all scales), and the velocity turbulent fluctuations at scales larger than the magnetic diffusion scale. The peak at $Q \approx 3$ for all $K$ in $\mathcal{T}_{ub}(Q, K)$ (the small-scale dynamo from the large-scale flow) also explains the development of the spectrum $\sim k^{3/2}$ for small wavenumbers in the magnetic energy spectrum at early times. It is worth remarking that this analysis gives only information of what are the sources of magnetic energy in each shell, for a given flow and at a given magnetic Reynolds number; the analysis of the shell-to-shell transfers gives no information on why different flows have different critical magnetic Reynolds (see e.g. [61, 65, 66]).

## 5. Conclusions

The results mentioned in the previous sections suggest that there are much stronger interactions between widely separated scales in turbulent MHD flows than in hydrodynamic flows. For a basic understanding of the MHD cascade processes, a simple order of magnitude estimation of the amplitude of the velocity and magnetic fields at each scale as well as assumptions of locality of interactions are not sufficient to reproduce all the observed results. Cross helicity and magnetic helicity also seem to play a dynamic role in the evolution of turbulent MHD flows, as was shown on a different basis in [69].

As a result, subgrid models need to take into account the long-range interactions and the correlations between fields in order to accurately predict the evolution of an MHD system. A turbulent eddy viscosity, for example, should depend on the different helicities of the flow and on the amplitude of the large-scale fields. Subgrid models, such as the Lagrangian averaged MHD equations (LAMHD) [70, 71] and rapid distortion theory (RDT) [12, 72] are promising in that respect.

Finally we would like to comment on the last question we posed in the introduction section: can we still pursue the search for a unique universal theory that describes MHD turbulence? The

evidence presented in this paper suggests that large-scale flows directly influence the small scales in MHD. During the kinematic regime of dynamo simulations this effect is even stronger [25], as was also known from theoretical studies [55] and numerical simulations [24] with magnetic Prandtl number larger than one. In section 3 it was also suggested that the saturation amplitude of the magnetic field in the large scales in helical flows can depend on the physical processes that control the reconnection events in the small scales. It is at least possible therefore that all turbulent MHD flows do not behave in the same way and one run does not span all possible statistical MHD turbulent configurations. An example of such behaviour is to be found in DNS of MHD turbulence in the presence of a uniform magnetic field [73].

However, we do not want to suggest that the only path is to perform separate high resolution numerical simulations for each MHD problem. On the contrary, we believe that there is a finite number of large-scale parameters (e.g. the helicity and cross helicity injection rates, the correlation time of the large-scale forcing, etc) and small-scale parameters (e.g. the Prandtl number) that control the behaviour of MHD turbulence in the inertial range and when kept fixed, universality classes can be unraveled, in much the same way as it was done for 2D Navier–Stokes turbulence [74]. These parameters and their effects however need yet to be fully determined. In that respect, different numerical simulations exploring parameter space will be of use.

## Acknowledgments

PDM acknowledges discussions with A A Schekochihin. Computer time was provided by NCAR. The NSF grant CMG-0327888 at NCAR supported this work in part and is gratefully acknowledged.

## References

[1] Balbus S A and Terquem C 2001 Linear analysis of the Hall effect in protostellar disks *Astrophys. J.* **552** 235–47

[2] Mininni P D, Gómez D O and Mahajan S M 2003 Dynamo action in magnetohydrodynamics and Hall-magnetohydrodynamics *Astrophys. J.* **587** 472–81

[3] Schekochihin A A, Cowley S C, Kulsrud R M, Hammett G W and Sharma P 2005 Plasma instabilities and magnetic field growth in clusters of galaxies *Astrophys. J.* **629** 139–142

[4] Moffatt H K 1978 *Magnetic Field Generation in Electrically Conducting Fluids* (Cambridge: Cambridge University Press)

[5] Wiltse J M and Glezer A 1993 Manipulation of free shear flows using piezoelectric actuators *J. Fluid Mech.* **249** 261–85

[6] Wiltse J M and Glezer A 1998 Direct excitation of small-scale motions in free shear flows *Phys. Fluids* **10** 2026–36

[7] Carlier J, Laval J P and Stanislas M 2001 Some experimental support at a high Reynolds number to a new hypothesis for turbulence modelling *C. R. Acad. Sci. Ser. II* **329** 35–40

[8] Poulain C, Mazellier N, Chevillard L, Gagne Y and Baudet C 2006 Dyamics of spatial Fourier modes in turbulence. Sweeping effect, long-time correlations and temporal intermittency *Eur. Phys. J.* B **53** 219–24

[9] Alexakis A, Mininni P D and Pouquet A 2005 Imprint of large-scale flows on turbulence *Phys. Rev. Lett.* **95** 264503

[10] Mininni P D, Alexakis A and Pouquet A 2006 Large-scale flow effects, energy transfer, and self-similarity on turbulence *Phys. Rev.* E **74** 016303

[11] Shen X and Warhaft 2000 The anisotropy of the small-scale structure in high Reynolds number ($r_\lambda \sim 1000$) turbulent shear flow *Phys. Fluids* **12** 2976–89
[12] Laval J-P, Dubrulle B and Nazarenko S 2001 Nonlocality and intermittency in three-dimensional turbulence *Phys. Fluids* **13** 1995–2012
[13] Iroshnikov P S 1963 Turbulence of a conducting fluid in a strong magnetic field *Sov. Astron.* **7** 566–71
[14] Kraichnan R H 1965 Inertial-range spectrum of hydromagnetic turbulence *Phys. Fluids* **8** 1385–7
[15] Matthaeus W H and Zhou Y 1989 Extended inertial range phenomenology of magnetohydrodynamic turbulence *Phys. Fluids* B **1** 1929–31
[16] Goldreich P and Sridhar P 1995 Toward a theory of interstellar turbulence. 2. Strong Alfvenic turbulence *Astrophys. J.* **438** 763–75
[17] Galtier S, Nazarenko S V, Newell A C and Pouquet A 2000 A weak turbulence theory for incompressible magnetohydrodynamics *J. Plasma Phys.* **63** 447–88
[18] Galtier S, Pouquet A and Mangeney A 2005 On spectral scaling laws for incompressible anisotropic magnetohydrodynamic turbulence *Phys. Plasmas* **12** 092310
[19] Boldyrev S 2006 Spectrum of magnetohydrodynamic turbulence *Phys. Rev.* E **96** 115002
[20] Verma M K 2004 Statistical theory of magnetohydrodynamic turbulence: recent results *Phys. Rep.* **401** 229–380
[21] Alexakis A, Mininni P D and Pouquet A 2005 Shell to shell energy transfer in MHD. I. Steady state turbulence *Phys. Rev.* E **72** 046301
[22] Debliquy O, Verma M K and Carati D 2005 Energy fluxes and shell-to-shell transfers in three-dimensional decaying magnetohydrodynamic turbulence *Phys. Plasmas* **12** 042309
[23] Yousef T A, Rincon F and Schekochihin A A 2007 Exact scaling laws and the local structure of isotropic magnetohydrodynamic turbulence *J. Fluid Mech.* **575** 111–20
[24] Schekochihin A A, Cowley S C, Taylor S F, Maron J L and McWilliams J C 2004 Simulations of the small-scale turbulent dynamo *Astrophys. J.* **612** 276–307
[25] Mininni P D, Alexakis A and Pouquet A 2004 Shell to shell energy transfer in MHD. II. Kinematic dynamo *Phys. Rev.* E **72** 046302
[26] Pouquet A, Frisch U and Léeorat J 1976 Strong MHD helical turbulence and the nonlinear dynamo effect *J. Fluid Mech.* **77** 321–54
[27] Meneguzzi M, Frisch U and Pouquet A 1981 Helical and nonhelical turbulent dynamos *Phys. Rev. Lett.* **47** 1060–4
[28] Brandenburg A 2001 The inverse cascade and nonlinear alpha-effect in simulations of isotropic helical hydromagnetic turbulence *Astrophys. J.* **550** 824–40
[29] Gómez D O and Mininni P D 2004 Direct numerical simulations of helical dynamo action: MHD and beyond *Nonlin. Process. Geophys.* **11** 619–29
[30] Alexakis A, Mininni P D and Pouquet A 2006 On the inverse cascade of magnetic helicity *Astrophys. J.* **640** 335–43
[31] Steenbeck M, Krause F and Rädler K-H 1966 Berechnung der mittleren Lorentz-Feldstaerke $\overline{\mathbf{v} \times \mathbf{b}}$ fuer ein elektrisch leitendendes Medium in turbulenter, durch Coriolis-Kraefte beeinflußter Bewegung *Z. Naturf. a* **21** 369–76
[32] Krause F and Raedler K-H 1980 *Mean-field Magnetohydrodynamics and Dynamo Theory* (New York: Pergamon)
[33] Dar G, Verma M K and Eswaran V 2001 Energy transfer in two-dimensional magnetohydrodynamic turbulence formalism and numerical results *Physica* D **157** 207–25
[34] Carati D, Debliquy O, Knaepen B, Teaca B and Verma M 2006 Energy transfers in forced MHD turbulence *J. Turbul.* **7** 1–12
[35] Domaradzki J A and Rogallo R S 1990 Local energy transfer and nonlocal interactions in homogeneous, isotropic turbulence *Phys. Fluids* **2** 413–26
[36] Ohkitani K and Kida S 1992 Triad interactions in a forced turbulence *Phys. Fluids* A **4** 794–802
[37] Zhou Y 1993 Interacting scales and energy transfer in isotropic turbulence *Phys. Fluids* A **5** 2511–24

[38] Yeung P K, Brasseur J G and Wang Q 1995 Dynamics of direct large-small scale couplings in coherently forced turbulence: concurrent physical- and Fourier-space views *J. Fluid Mech.* **283** 43–95
[39] Mason J, Cattaneo F and Boldyrev S 2006 Dynamic alignment in driven magnetohydrodynamic turbulence *Phys. Rev. Lett.* **97** 255002
[40] Field G B and Blackman E G 2002 Dynamical quenching of the alpha dynamo *Astrophys. J.* **572** 685–92
[41] Blackman E G 2004 Bihelical magnetic relaxation and large scale magnetic field growth *Phys. Plasmas* **12** 012304
[42] Frisch U, Pouquet A, Léorat J and Mazure A 1975 Possibility of an inverce cascade of magnetic helicity in hydrodynamic turbulence *J. Fluid Mech.* **68** 769–78
[43] Pouquet A and Patterson G S 1978 Numerical simulation of helical magnetohydrodynamic turbulence *J. Fluid Mech.* **85** 305–23
[44] Kida S, Yanase S and Mizushima J 1991 Statistical properties of MHD turbulence and turbulent dynamo *Phys. Fluids* A **3** 457–65
[45] Low B C 1994 Magnetohydrodynamic processes in the solar corona: flares, coronal mass ejections, and magnetic helicity *Phys. Fluids* **1** 1684–90
[46] Low B C and Berger M A 2003 A morphological study of helical coronal magnetic structures *Astrophys. J.* **589** 644–57
[47] Mandrini C H, Démoulin P, van Driel-Gesztelyi L and López Fuentes M C 2004 Magnetic helicity budget of solar-active regions from the photosphere to magnetic clouds *Astrophys. Space Sci.* **290** 319–44
[48] Gibson S E, Fan Y, Mandrini C, Fisher G and Demoulin P 2004 Observational consequences of a magnetic flux rope emerging into the corona *Astrophys. J.* **617** 600–13
[49] Démoulin V 2007 Recent theoretical and observational developments in magnetic helicity studies *Adv. Space Res.* at press
[50] Berger M A and Ruzmaikin A 2000 Rate of helicity production by solar rotation *J. Geophys. Res.* **105** 10481–90
[51] Brandenburg A and Subramanian K 2005 Astrophysical magnetic fields and nonlinear dynamo theory *Phys. Rep.* **417** 1–209
[52] Zel'Dovich Ya B, Ruzmaikin A A and Sokoloff D D 1983 *Magnetic Fields in Astrophysics* (New York: Gordon and Breach)
[53] Schekochihin A A, Maron J L, Cowley S C and McWilliams J C 2002 The small-scale structure of magnetohydrodynamic turbulence with large magnetic Prandtl numbers *Astrophys. J.* **576** 806–13
[54] Haugen N E L, Brandenburg A and Dobler W 2004 Simulations of nonhelical hydromagnetic turbulence *Phys. Rev.* E **70** 016308
[55] Zel'Dovich Ya B, Ruzmaikin A A, Molchanov S A and Sokoloff D D 1984 Kinematic dynamo problem in a linear velocity field *J. Fluid Mech.* **144** 1–11
[56] Schekochihin A A, Cowley S C, Hammett G W, Maron J L and McWilliams J C 2002 A model of nonlinear evolution and saturation of the turbulent mhd dynamo *New J. Phys.* **4** 84
[57] Kazanstev A P 1968 Enhancement of a magnetic field by a conducting fluid *Sov. Phys. JETP* **26** 1031–4
[58] Ponty Y, Mininni P D, Montgomery D C, Pinton J-F, Politano H and Pouquet A 2005 Numerical study of dynamo action at low magnetic Prandtl numbers *Phys. Rev. Lett.* **94** 164502
[59] Mininni P D and Montgomery D C 2005 Low magnetic Prandtl number dynamos with helical forcing *Phys. Rev.* E **72** 056320
[60] Mininni P D 2006 Turbulent magnetic dynamo excitation at low magnetic Prandtl number *Phys. Plasmas* **13** 056502
[61] Frick P, Stepanov R and Sokoloff D 2006 Large- and small-scale interactions and quenching in an $\alpha^2$-dynamo *Phys. Rev.* E **74** 066310
[62] Mininni P D, Ponty Y, Montgomery D C, Pinton J-F, Politano H and Pouquet A 2005 Dynamo regimes with a nonhelical forcing *Astrophys. J.* **626** 853–63
[63] Schekochihin A A, Haugen N E L, Brandenburg A, Cowley S C, Maron JL and McWilliams J C 2005 The onset of a small-scale turbulent dynamo at low magnetic Prandtl numbers *Astrophys. J.* **625** L115–8

[64] Iskakov A B, Schekochihin A A, Cowley S C, McWilliams J C and Proctor M R E 2007 Numerical demonstration of fluctuation dynamo at low magnetic prandtl numbers *Phys. Rev. Lett.* at press (*Preprint* astro-ph/0702291)
[65] Vincenzi D 2002 The Kraichnan–Kazantsev dynamo *J. Stat. Phys.* **106** 1073–91
[66] Boldyrev S and Cattaneo F Magnetic-field generation in Kolmogorov turbulence *Phys. Rev. Lett.* **92** 144501
[67] Galanti B, Sulem P-L and Pouquet A 1992 Linear and nonlinear dynamos associated with ABC flows *Geophys. Astrophys. Fluid Dyn.* **66** 183–208
[68] Moffatt K 1961 The amplification of a weak applied magnetic field by turbulence in fluids of moderate conductivity *J. Fluid Mech.* **11** 625–35
[69] Ting A C, Matthaeus W H and Montgomery D 1986 Turbulent relaxation processes in magnetohydrodynamics *Phys. Fluids* **29** 3261–74
[70] Holm D D 2002 Lagrangian averages, averaged Lagrangians, and the mean effects of fluctuations in fluid dynamics *Chaos* **12** 518–30
[71] Mininni P D, Montgomery D C and Pouquet A 2005 A numerical study of the alpha model for two-dimensional magnetohydrodynamic turbulent flows *Phys. Fluids* **17** 035112
[72] Dubrulle B, Laval J-P, Nazarenko S and Zaboronski O 2004 A model for rapid stochastic distortions of small-scale turbulence *J. Fluid Mech.* **520** 1–21
[73] Müller W C and Grappin R 2005 Spectral energy dynamics in magnetohydrodynamic turbulence *Phys. Rev. Lett.* **95** 114502
[74] Bernard D, Boffetta G, Celani A and Falkovich G 2006 Conformal invariance in two-dimensional turbulence *Nat. Phys.* **2** 124–8